

Article

Shear Strengthening and Repairing of Reinforced Concrete Deep Beams Damaged by Heat Using NSM–CFRP Ropes

Ahmad Al-khreisat ², Mu'tasime Abdel-Jaber ^{1,2,*} and Ahmed Ashteyat ²

¹ Faculty of Engineering, Department of Civil Engineering, Al-Ahliyya Amman University, Amman 19328, Jordan

² Faculty of Engineering, Department of Civil Engineering, The University of Jordan, Amman 11942, Jordan

* Correspondence: m.abduljaber@ju.edu.jo

† On sabbatical leave from the Department of Civil Engineering, The University of Jordan, Amman 11942, Jordan.

Abstract: This study investigates experimentally the shear strengthening and repairing of reinforced concrete (RC) deep beams damaged by heat utilizing near-surface mounted carbon fiber reinforced polymers (NSM-CFRP) ropes. The main parameters adopted in this research are rope orientation (45°, 90°) and rope spacing (150 mm, 200 mm). For this purpose, ten RC deep beams were cast and tested until failure was reached. The test results showed that using NSM-CFRP ropes with various configurations significantly enhanced the shear capacity for repaired and strengthened deep beams. All the tested beams enhanced the ultimate load capacity for the strengthened beams ranging between 19% to 46%, while for the repaired beams, the values ranged between 40.8% to 64.6%. The CFRP ropes oriented at 45° recorded the highest enhancement result in shear capacity. Notably, all tested beams had a satisfactory rise in the enhancement ratio. Consequently, the economic aspect should have priority.

Keywords: deep beams; shear strengthening; near-surface mounted; CFRP ropes



Citation: Al-khreisat, A.; Abdel-Jaber, M.; Ashteyat, A. Shear Strengthening and Repairing of Reinforced Concrete Deep Beams Damaged by Heat Using NSM–CFRP Ropes. *Fibers* **2023**, *11*, 35. <https://doi.org/10.3390/fib11040035>

Academic Editors: Constantin Chalioris and Dae-jin Kim

Received: 13 February 2023

Revised: 30 March 2023

Accepted: 10 April 2023

Published: 13 April 2023



Copyright: © 2023 by the authors. Licensee MDPI, Basel, Switzerland. This article is an open access article distributed under the terms and conditions of the Creative Commons Attribution (CC BY) license (<https://creativecommons.org/licenses/by/4.0/>).

1. Introduction

Reinforced concrete (RC) structural components are designed to withstand a multitude of loads. However, due to water vapor pressure and the uneven thermal reaction of aggregate and hydrated cement, various structural components may be exposed to high temperatures due to fire outbreaks, leading to radical and unwanted changes in the concrete's physical, chemical, and mechanical properties [1,2].

Depending on the temperature, several types of damage may occur to concrete. Reduced compressive strength, microcracking in the concrete microstructure, color changes indicative of decreased strength, increased pore structure, and varying degrees of spalling were the results of exposing concrete components to high temperatures. After being subjected to high temperatures, concrete retains its compressive strength in three stages, with the first stage occurring when the temperature is between 300 °C and room temperature. The concrete's compressive strength began to significantly decline between 300 and 800 °C, and it completely disappeared at temperatures above 800 °C [3–6].

The following paragraph demonstrates how the CFRP strategy successfully increases the ultimate strength of RC beams, focusing on the shear behavior of RC beams that have been repaired using the NSM-CFRP technique [7–21]. Ibrahim et al. [22] showed that NSM-CFRP could increase the shear capacity of the RC beams by 55.8% and strengthen the connection between concrete and FRP materials. Abdallah et al. [23] showed that RC beams might be strengthened using NSM-FRP to increase their overall load-carrying capacity and yielding loads with a minimal loss in ductility. Abdel-Jaber et al. [24] found that employing NSM-CFRP strips can significantly enhance the shear capacity of RC beams by 66%. Dias et al. [25] examined the NSM-CFRP laminates technique's efficacy in strengthening

RC beams under shear. They observed that the shear strengthening of RC beams might be achieved effectively by employing NSM-CFRP laminates. Jalali et al. [26] examine the effectiveness of NSM-CFRP rods for RC beam shear strengthening. They found that using NSM-CFRP rods increased the shear capacity of RC beams to 48%. Mansour et al. [27] conducted an investigational program, including experiments to monitor the progress of RC deep beams strengthened with NSM-CFRP around cutouts. They found that the NSM-CFRP strips could improve the interlocking of the aggregate contribution to shear resistance. When the number of strips in ties was doubled, the shear resistance remained unchanged noticeably because the aggregate interlock's impact on the shear resistance was negligible. Al-Issawi et al. [28] performed a study to test the accomplishment of RC deep beams strengthened by near-surface mounted steel bars. Thirteen specimens were cast and given additional support from steel bars using various strengthening techniques. Albidah et al. [29] executed an experiment program to assess the efficacy of RC deep beam strengthening techniques with fiber-reinforced polymer (FRP) material. Strengthening initiatives increased the deep beams' shear strength, although they reduced the beam's capacity for deformation. Due to the absence of coherence in the interfacial zone between the FRP material and concrete surface, premature debonding limits the retrofitting effectiveness of the FRPs in RC structures, resulting in a lower real strain response relative to the entire potential intended capacity. Additionally, numerous studies already conducted and published in the larger body of literature have shown that premature debonding or delamination of the FRP layer from the concrete substrate is the most common failure mode of reinforced RC members with externally epoxy-bonded FRP composites. The aforementioned event is brought on by a high concentration of stress and is followed by brittle catastrophic collapse. The presence of the slab limits the applicability of wrapping the FRP retrofitting materials around the cross-section and/or accessibility to properly apply the end anchorage, which leads to the early debonding failure of the externally applied FRP, especially in T-shaped RC structural members and U-shaped strengthening scheme applications [30–32].

Using the NSM approach to strengthen and repair beams subjected to high temperatures has been experimentally examined by several researchers [33–38]. Jiangtao et al. [39] studied the behavior of 15 RC beams that had been reinforced with NSM-CFRP and had been subjected to high-load fire exposure for more than three hours. The retrofitted beams could sustain the conventional fire for a period of time greater than three hours at such a heavy load level. Al-Rousan [40] investigated the effectiveness of employing NSM-CFRP strips as the main or secondary shear reinforcement after exposure to high heat. The test research found that CFRP strips may be used satisfactorily in RC beams subjected to intense heat as external shear reinforcement.

CFRP ropes are affordable materials that have lately been utilized to reinforce RC deep beams that were not exposed to heat. However, the repairing of RC beams with heat damage using CFRP ropes has not really been done. Therefore, research is scarce on the most effective strengthening and repair approach for retrofitting the RC deep beams exposed to high temperatures. This investigation intends to repair and strengthen RC deep beams exposed to heat damage utilizing NSM-CFRP ropes. In this study, RC beams subjected to a high temperature of 650 °C for three hours are investigated. A total of 10 RC deep beams were cast, five of the beams were subjected to 650 °C for three hours, and the remaining five beams were left unheated; CFRP ropes were subsequently used to strengthen the remaining four unheated specimens and to repair four heat-damaged beams. Of the two control beams, one was heated and the other left at room temperature. All the tested beams were designed using the requirements of the American Concrete Institute's Code for Model of Strut-and-Tie (ACI 318M-19) [41–45].

2. Experimental Program

2.1. Materials

Table 1 shows the mix design. Ropes made of CFRP were used to reinforce the specimens. The mechanical and physical features of the CFRP ropes are shown in Table 2.

A total of two types of resin in this experimental study, Sikadur[®]-330, and Sikadur[®]-52 LP, were used. Table 3 shows the mechanical and physical features of the resin used. SikaWrap FX-50 C, Sikadur[®]-330, and Sikadur[®]-52 LP were obtained from Sika company, UAE, and the concrete mix was obtained from Almanaseer company, (Amman, Jordan).

Table 1. Concrete mix design.

Material	Weight
Cement (OPC)	223 kg
Coarse Aggregate	338 kg
Medium Aggregate	636 kg
Total water	185 kg
Net water	168 kg
Total Aggregate	1987 kg
Density	2342 kg/m ³
Water to cement ratio(w/c)	0.75

Table 2. NSM- CFRP ropes properties.

Properties	SikaWrap FX-50 C
Material Type	Unidirectional high-strength carbon fiber strand in a plastic sleeve
Fibre Density (g/cm ³)	1.82
Tensile Strength (MPa)	4000
Cross Section (mm ²)	≥28
Modules of Elasticity (GPa)	240
Mass per Unit Length (g/m)	≥50
Elongation at Break (%)	≥1.6

Table 3. Epoxy Adhesive Properties.

Resin Type/Property	Sikadur [®] -330	Sikadur [®] -52 LP
	Resin: part A (white) Hardener: part B (grey)	Resin: part A (Transparent) Hardener: part B(Brownish)
Packaging	5 kg A + B (light grey)	4 kg A + B (Yellowish brownish)
Density	1.3 ± 0.1 kg/L	1.06 kg/L
Tensile Strength	30 N/mm ²	~27 N/mm ²
Mixing Ratio	Part A:Part B = 4:1 (by weight)	A:B = 2:1 part by weight and by volume
Elongation at break	0.9%	1.9%

2.2. Specimens Details

A total of 10 RC deep beams were cast and tested under two loading points with a shear span-to-depth ratio of 1.44, with cross-sectional dimensions of 190 mm width, 450 mm depth, and an overall length of 1900 mm, as shown in Figure 1. All beams were designed to fail in shear rather than flexure. As a result, each beam was primarily strengthened at the bottom with six 16 mm diameter bars placed in two layers to resist the resulting bending moment, while shear reinforcements were not presented.

RC deep beams repaired with NSM CFRP ropes were investigated in the five beams that had been heated to determine the impact of temperature. The other five samples weren't heated. NSM CFRP ropes were used to repair and strengthen RC specimens. Table 4 shows details about the test specimens.

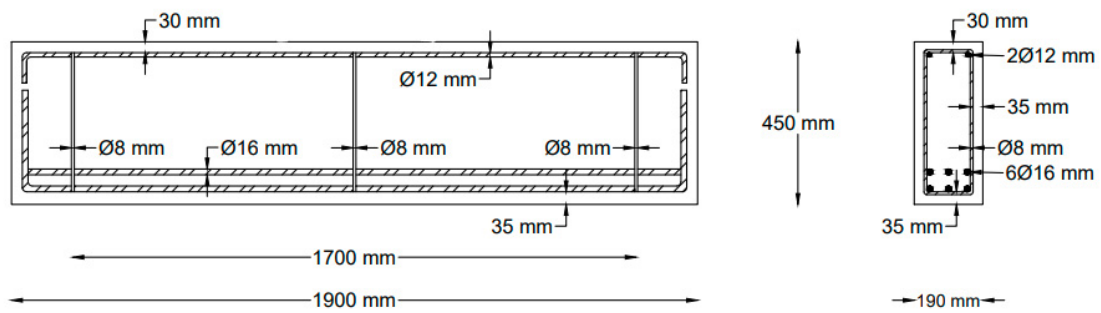


Figure 1. Specimens details.

Table 4. Beams details.

Group NO.	Beams ID	CFRP Ropes Spacing (mm)	CFRP Ropes Inclination	Heated/ Un-Heated	Strengthening Layout Based on Figure 2
1	CA-1	-	-	Unheated	-
	SB-150mm@45°	150 mm	45°	Unheated	A
	SB-200mm@45°	200 mm	45°	Unheated	B
	SB-150mm@90°	150 mm	90°	Unheated	C
	SB-200mm@90°	200 mm	90°	Unheated	D
2	CA-2	-	-	Heated	-
	HB-150mm@45°	150 mm	45°	Heated	A
	HB-200mm@45°	200 mm	45°	Heated	B
	HB-150mm@90°	150 mm	90°	Heated	C
	HB-200mm@90°	200 mm	90°	Heated	D

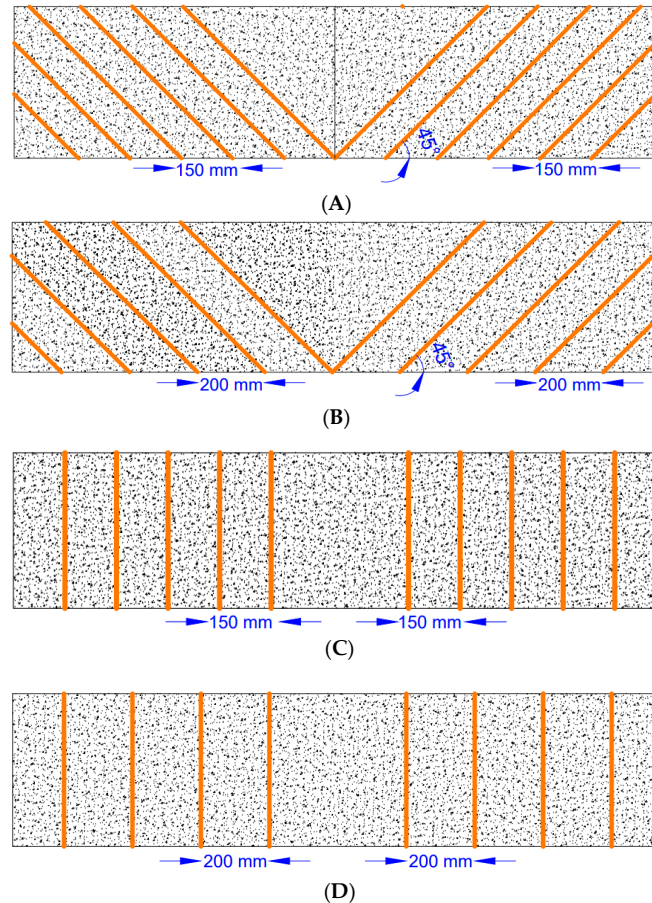


Figure 2. Strengthening configurations.

2.3. Heat Application

Before the repairing process, five beams were subjected to 650 °C for three hours in normal air conditions, and five beams were left unheated. The four unheated RC specimens were strengthened using NSM-CFRP ropes. Heat-damaged beams were repaired using NSM-CFRP ropes, and of two control beams, one was heated and the other left at room temperature.

A fabricated high-temperature furnace is employed to provide heat to the specimens. The internal dimensions of the furnace are 2 m × 2.5 m × 0.8 m, and it is covered by a 2.2 m × 2.7 m steel slab cover, as shown in Figure 3. The heat is monitored until it reaches 650 °C, and the heating time is kept for three hours after reaching this temperature. The specimens can be cooled down using either the fast way, submerging the specimens into water, or as applied here, which is leaving them in the air for one day.



Figure 3. Furnace Dimensions.

2.4. Installation of NSM-CFRP Ropes

The beams with the above-specified dimensions were identified to each take a certain dimension of the grooves. An electric saw was used to create the groove, which was 15 mm wide by 20 mm thick, as shown in Figure 4. To ensure a precise connection between the concrete and the epoxy resin, all of the dust was subsequently eliminated using an air blower. To partially fill the groove, in agreement with the manufacturer's instructions, the epoxy resin was created. It can be seen that the surrounding area of the groove was contaminated with epoxy resin, but it was surficial and had no effect on the mechanical performance. The manufacturer's recommended mix ratio was used to evenly combine both parts of the epoxy resin before applying it throughout the whole surface at the specified thickness. Following the installation of the carbon fiber, specialized tools were used to level the surface. According to the NSM-technical CFRP's specifications, the specimens were tested a week following the NSM-CFRP installation, after the epoxy already had time to cure and gained strength. The installation of NSM-CFRP and the groove preparation are shown in Figure 5.

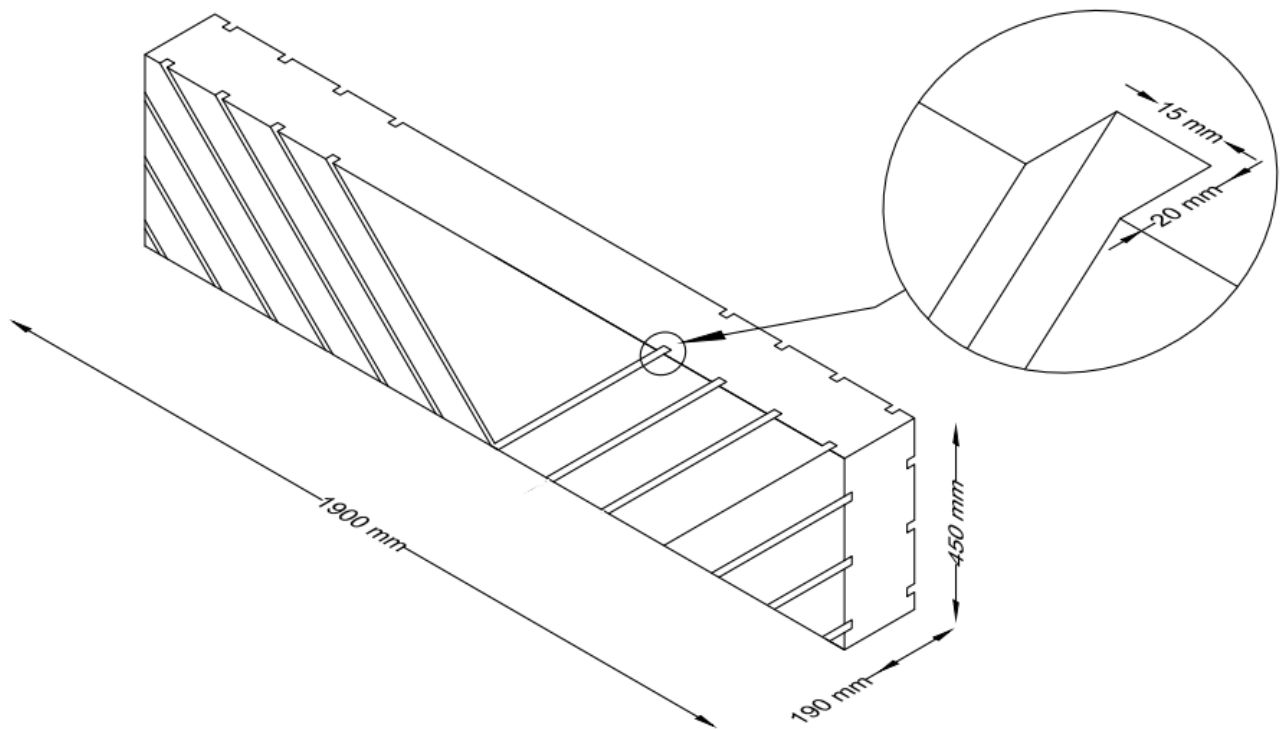


Figure 4. Groove Dimensions.



(a)



(b)

Figure 5. NSM-CFRP installation: (a) preparation of groove and (b) NSM-CFRP installation.

2.5. Test Setup

A total of 10 specimens were tested under two loading points applied to simply supported deep beams. Each beam had a steel roller supporting it at either end, and each support was spaced 100 mm from the end of the beam. A total of two symmetrically concentrated loads were applied to the tested beams at a total spaced distance of 400 mm, each positioned at a certain distance from the beam's center. As illustrated in Figure 6, the shear span to depth ratio for each of the beam specimens was maintained at 1.44 by applying one of the two concentrated loads 650 mm from the center of the right support and the other concentrated load at the same distance from the center of the left support. A linear variable displacement transducers (LVDT) device was installed at the bottom of the beam to measure the vertical mid-span deflection during the test, as displayed in Figure 6.

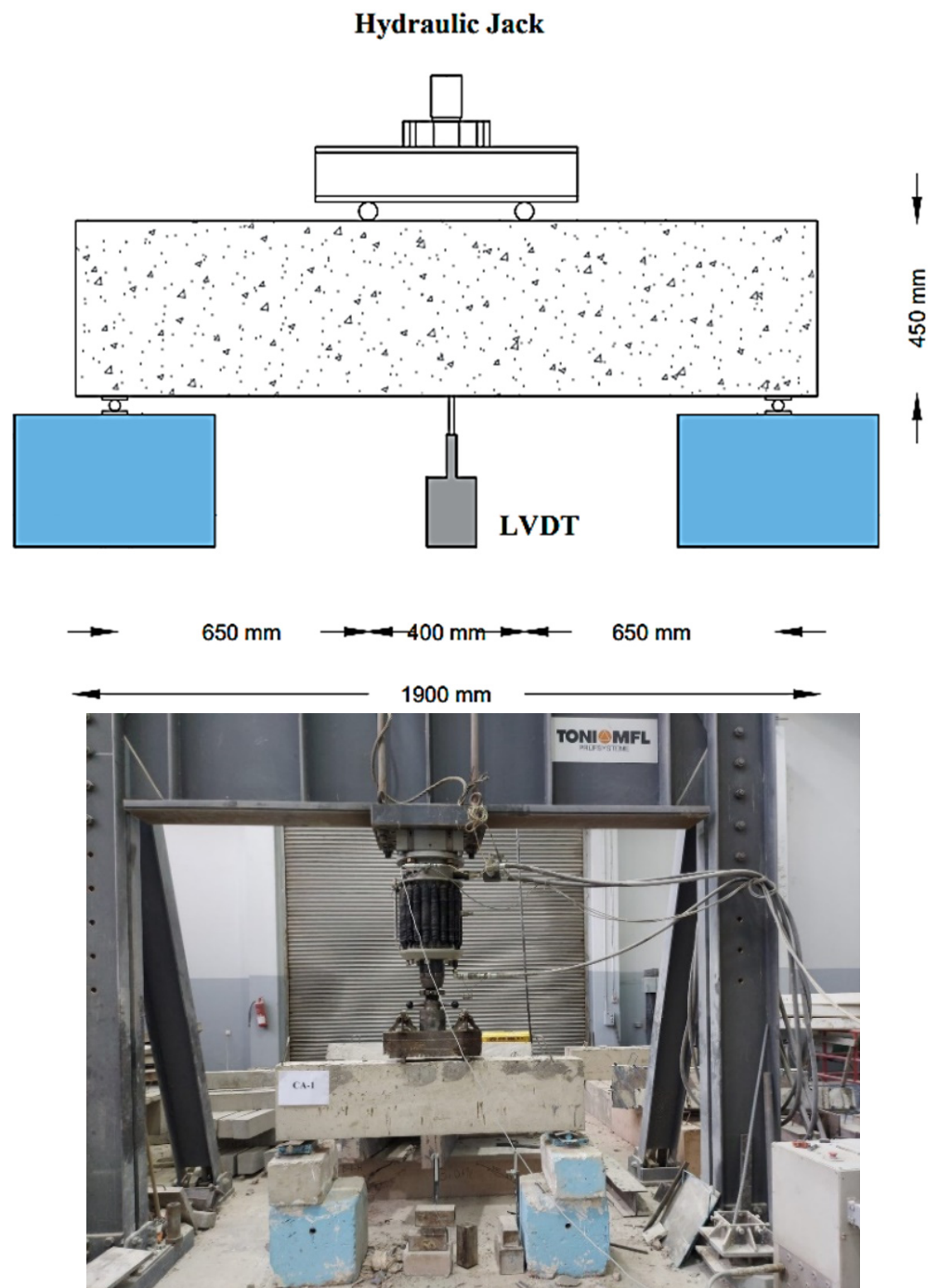


Figure 6. Test setup.

3. Test Results and Discussions

This section discusses the test outcomes in terms of load-deflection curves and failure mechanisms. Table 5 provides a list of the experiment results. The unheated specimens are denoted by the notation S. In contrast, the heat-damaged specimens are denoted by the notation H. Table 5 compares the behavior of the tested beams concerning the control unheated beam CA-1.

Table 5. Test results.

Specimen ID	Ultimate Load (kN)	Variation Percentages in Ultimate Load Compared to Unheated CA-1	Peak Displacement (mm)	%Peak Displacement (mm)	Failure Mode
CA-1 (control)	322	-	7.71	-	Shear failure
SB-150mm@45°	471	46%	9.53	23%	Shear failure
SB-200mm@45°	478	48%	13.33	73%	Shear failure
SB-150mm@90°	443	38%	9.77	27%	Shear failure
SB-200mm@90°	383	19%	9.29	20%	Shear failure
CA-2(heat damaged control)	257	−20%	10	30%	Shear failure
HB-150mm@45°	423	31%	10.8	40%	Shear failure
HB-200mm@45°	383	19%	9.5	23%	Shear failure
HB-150mm@90°	362	12%	8.52	11%	Shear failure

Control specimens

In this study, two control samples were tested. Specimen CA-1 was tested at 23 °C, whereas specimen CA-2 was heated before being evaluated at room temperature. The load-deflection curves for all beams are shown in Figure 7. Peak loads of specimens CA-1 and CA-2 are 322 kN and 257 kN, correspondingly, whereas peak displacements of the beams are 7.71 mm and 10 mm, respectively. The control specimen's load-carrying capacity was 20% reduced after exposure to 650 °C. Figure 12a,b show that shear failure happened in both specimens.

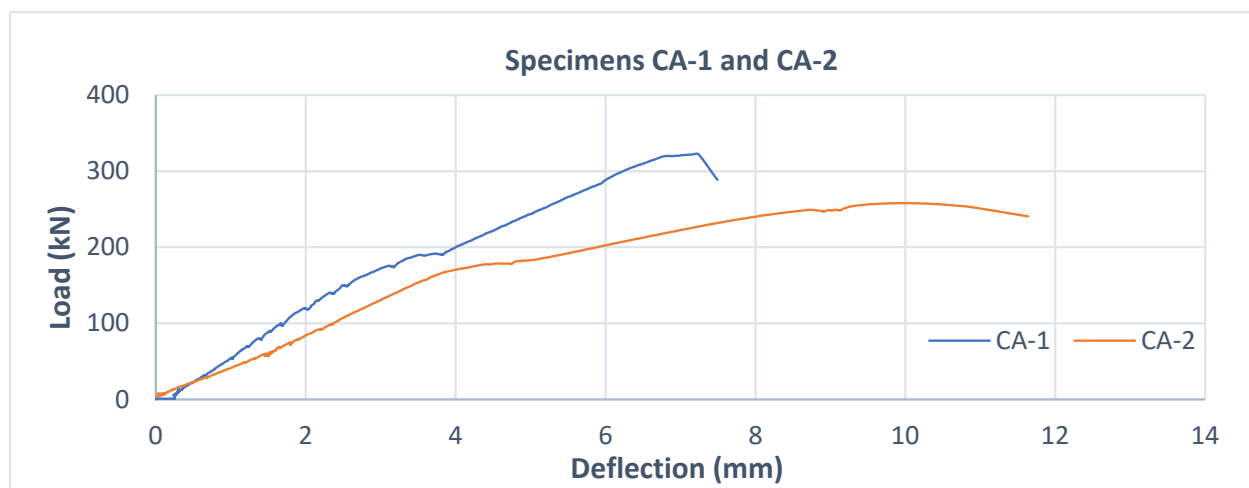


Figure 7. Load-deflection curve for Specimens CA-1 and CA-2.

Specimen (SB-150mm@45°) and (HB-150mm@45°)

CFRP ropes spaced at 150 mm and oriented at 45° were used to strengthen these two samples. The sole difference that sets them apart is that specimen HB-150mm@45° was tested after exposure to heat reaching 650 °C for three hours and repaired with CFRP ropes. CFRP ropes were used to strengthen the SB-150mm@45° specimen before tests were conducted without heat. Figure 12c,d show that shear failure happened in both specimens. The ultimate load for specimen SB-150mm@45° is 471 kN, compared to specimen HB-150mm@45° ultimate load of 423 kN. The ultimate capacity of the heat-damaged specimen HB-150mm@45° was recovered using CFRP ropes, which increased that capacity by up

to 31% compared to the control specimen CA-1. Consequently, a 46% increase in load-bearing capacity was noticed when comparing the identical control beam to the unheated SB-150mm@45° beam using CFRP ropes. For both specimens, Figure 8 displays the load-deflection curves.

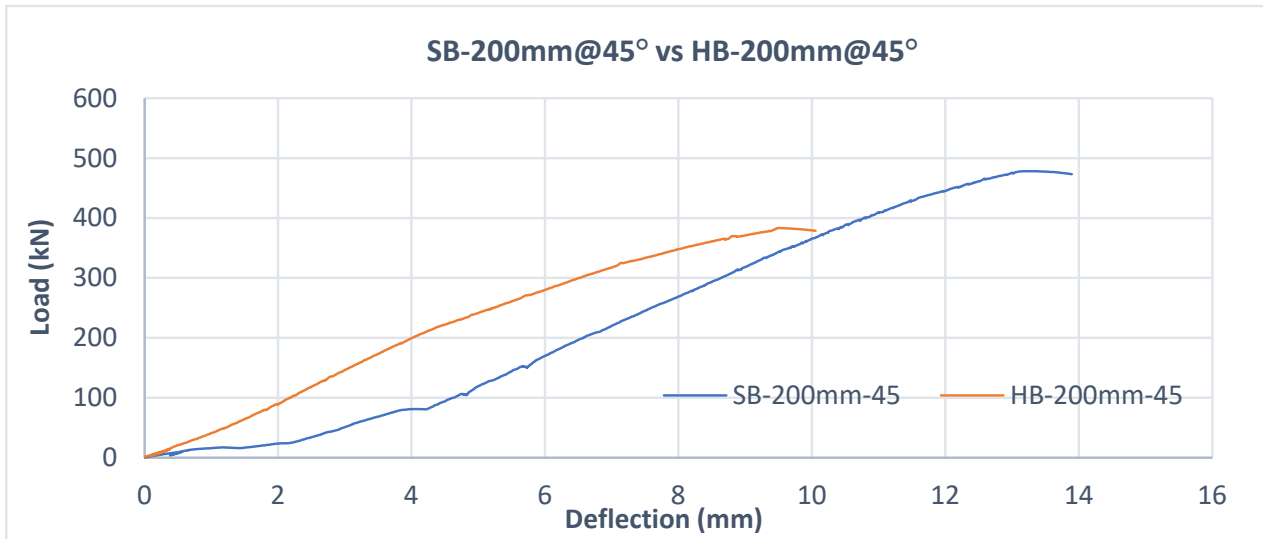


Figure 8. Load-deflection curve for Specimens SB-150mm@45° and HB-150mm@45°.

Specimen (SB-200mm@45°) and (HB-200mm@45°)

CFRP ropes spaced at 200 mm and oriented at 45° were used to strengthen these two samples. The only difference is that specimen HB-200mm@45° was tested after exposure to heat reaching 650 °C for three hours and repaired with CFRP ropes. CFRP ropes were used to strengthen the SB-200mm@45° specimen before tests were conducted without heat. Figure 12e,f show that shear failure happened in both specimens. The ultimate load for specimen SB-200mm@45° is 478 kN, compared to specimen HB-200mm@45° ultimate loads of 383 kN. The capacity of the heat-damaged specimen HB-200mm@45° was recovered using CFRP ropes, which increased that capacity by up to 19% compared to the control specimen CA-1. Consequently, a 48% increase in load-bearing capacity was noticed when comparing the identical control beam to the unheated SB-200mm@45° beam using CFRP ropes. For both specimens, Figure 9 displays the load-deflection curves.

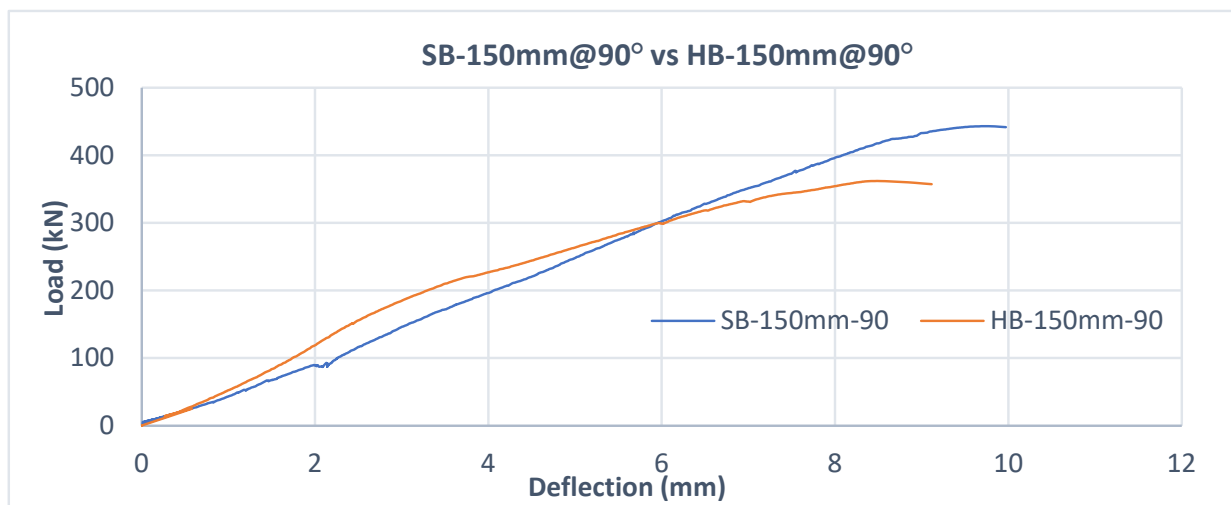


Figure 9. Load-deflection curve for Specimens SB-200mm@45° and HB-200mm@45°.

Specimen (SB-150mm@90°) and (HB-150mm@90°)

These two samples were strengthened using CFRP ropes at a configuration of 90 degrees inclination and a spacing of 150 mm. The load-deflection curves for both specimens are shown in Figure 10. According to the test findings, the specimens SB-150mm@90° and HB-150mm@90° had greater ultimate load capacities than the control beam CA-1 by 38% and 12%, respectively. Figure 12g,h show that shear failure happened in both specimens.

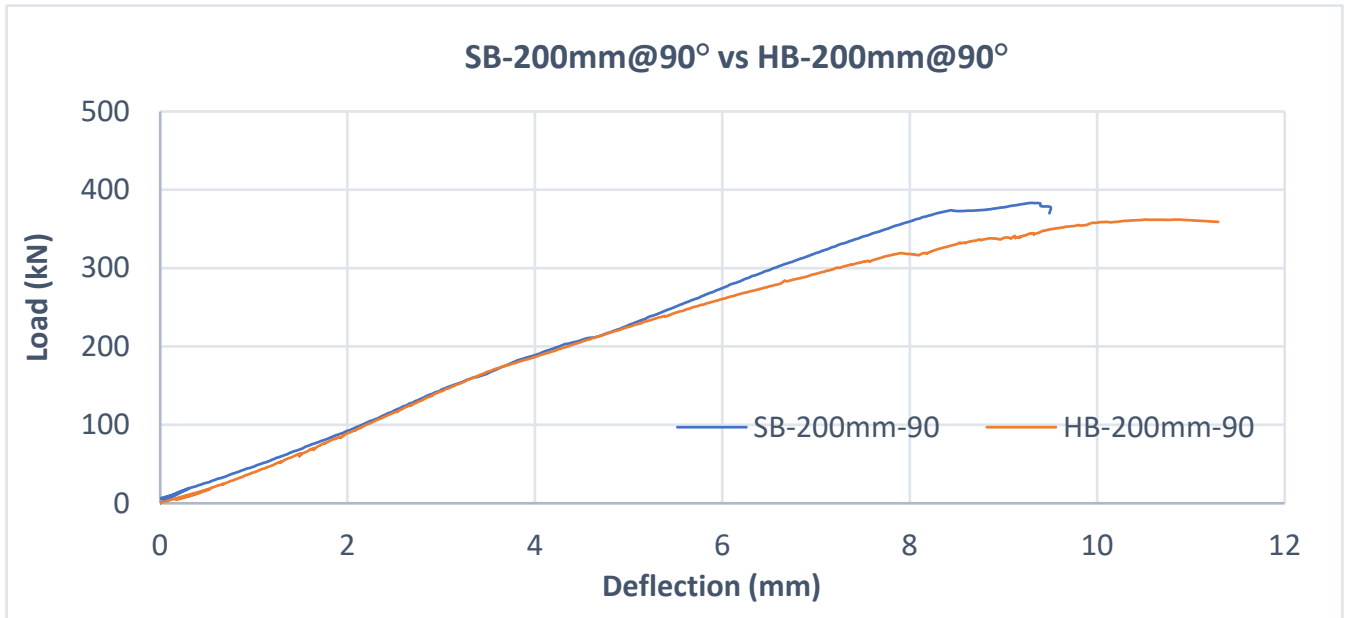


Figure 10. Load-deflection curve for Specimens SB-150mm@90° and HB-150mm@90°.

Specimen (SB-200mm@90°) and (HB-200mm@90°)

Both specimens were strengthened using CFRP ropes at a configuration of 90 degrees inclination and a spacing of 200 mm. For both specimens, the load-deflection curves are shown in Figure 11. In contrast to the control beam CA-1, the test results demonstrated an increase in the ultimate load capacity of specimens SB-200mm-90° and HB-200mm-90° of 19% and 12%, respectively. Shear failure happened in both specimens, as shown in Figure 12i,j.

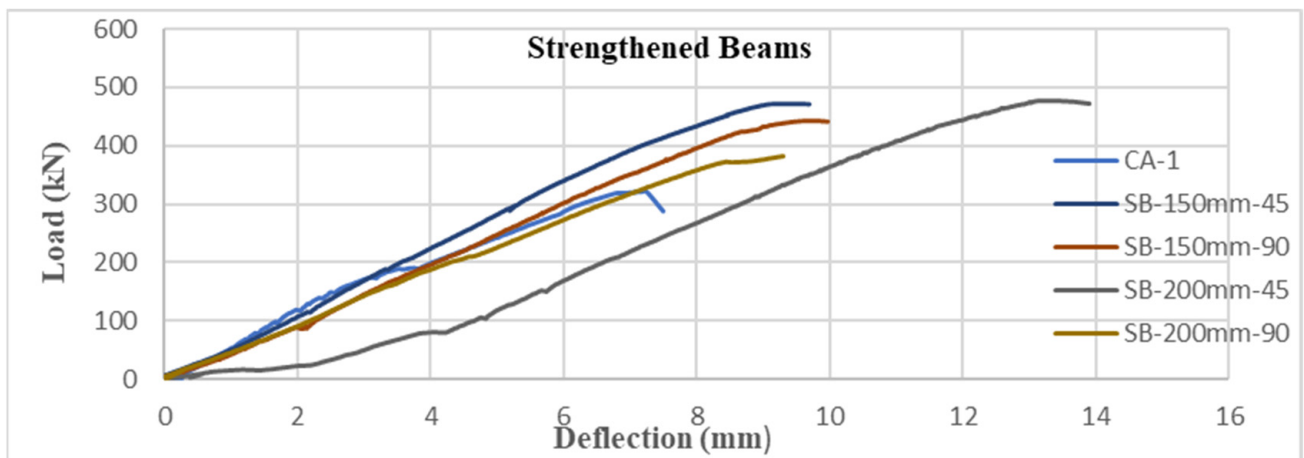


Figure 11. Load-deflection curve for Specimens SB-200mm@90° and HB-200mm@90°.

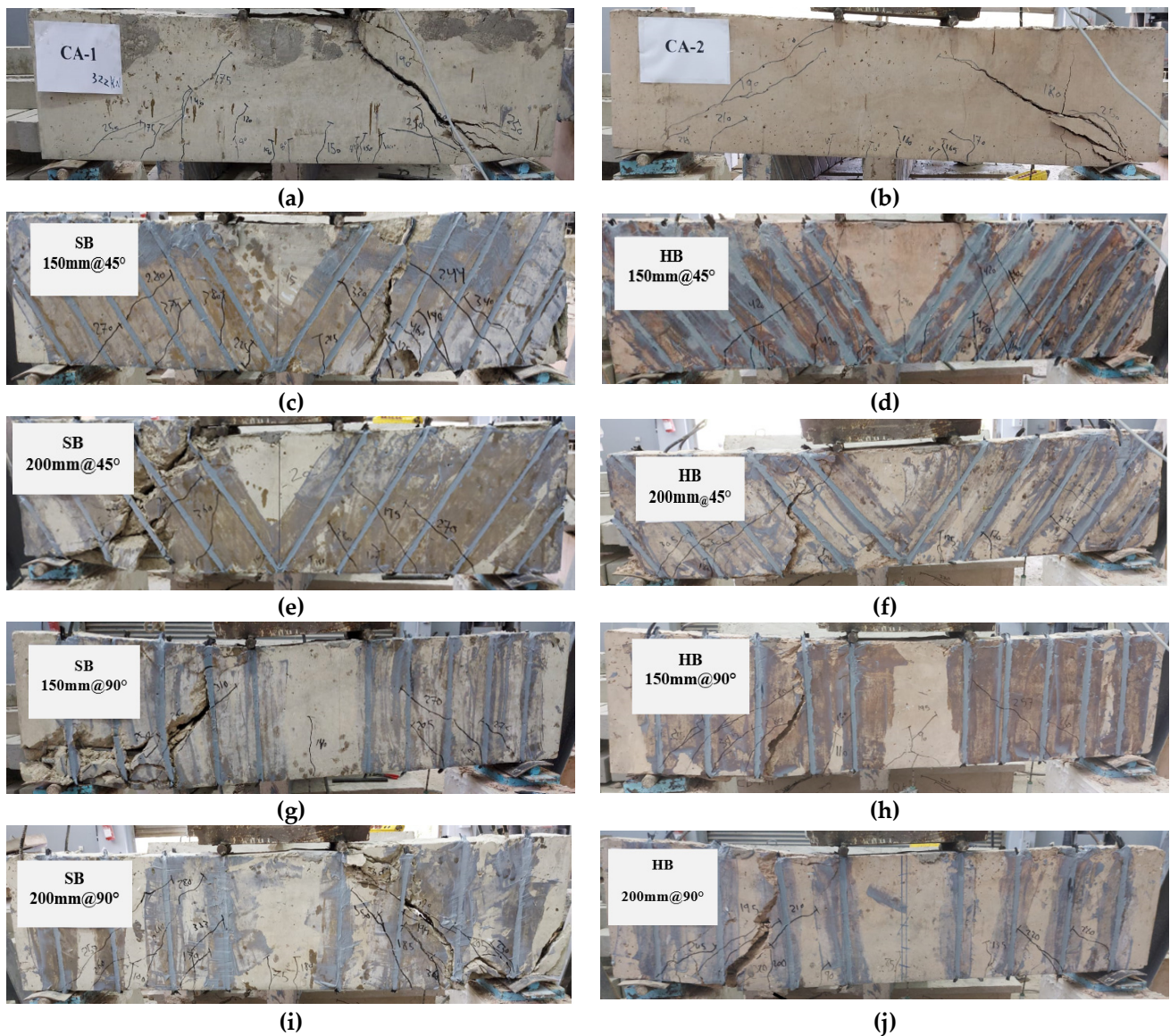


Figure 12. Failure modes of RC beams.

4. Effect of NSM-CFRP Ropes Configuration

This section will explore the impacts of different configurations on the shear strength of the enhanced RC deep beams utilizing NSM-CFRP ropes.

4.1. Effect of NSM-CFRP Ropes on Strengthened Beams

The ultimate load capacity of the strengthened beams conveyed a rise in the load capacity compared to control beam CA-1 by 48%, 46%, 38%, and 19% for SB-200mm@45°, SB-150mm@45°, SB-150mm@90°, SB-200mm@90° respectively. Furthermore, shear failure with concrete crushing was the most common failure mechanism in all specimens, adding to the partial debonding of the CFRP ropes and cover separation in certain beams. Figure 13 shows the load-deflection curve for strengthened beams.

As demonstrated in Figure 14, the ultimate load capacity was succeeded with beam SB-200mm@45° which achieved the best strengthening scheme at an enhancement ratio of 48% where the CFRP ropes were oriented at 45° at a spacing of 200 mm. On the contrary, beam SB-200mm@90° with an enhancement ratio of 19% oriented at 90° to a spacing of 200 mm had the lowest strengthening result, although it also maintained a positive increase on the overall strength of the beam. This indicates that strengthening using CFRP ropes

oriented at 45° at a spacing of 200mm had the best outcome. It should be noted that in this particular orientation, the two different spacings had extremely close results, which would indicate that spacing doesn't make a big difference in a 45° oriented beam. On the other hand, when CFRP ropes are oriented at 90°, the spacing made a difference as the spacing of 150 mm had a higher enhancement ratio compared to 200 mm spacing which indicates that at 90° orientation, installing CFRP ropes closer achieved better results. Consequently, strengthening utilizing CFRP ropes improved the ductility behavior as all reinforced beams displayed a rise in deflection compared to the CA-1 control beam.

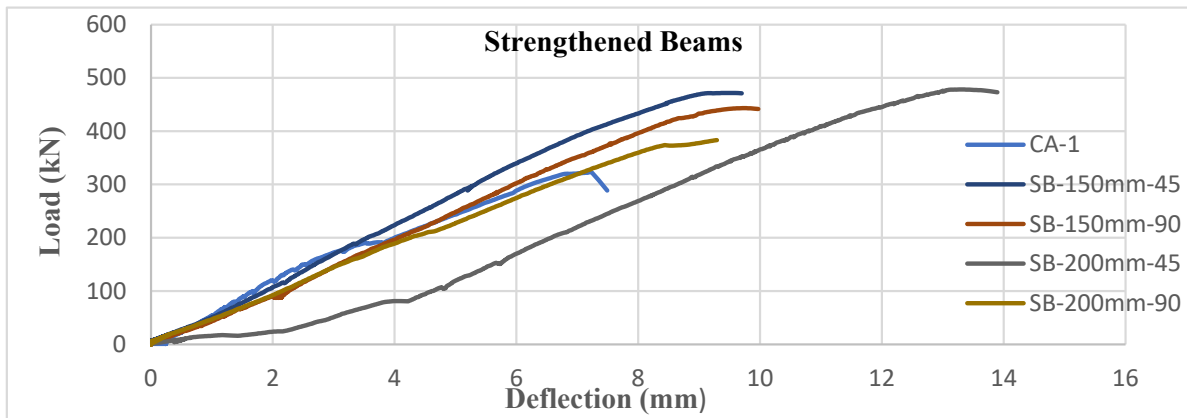


Figure 13. The load-deflection curve for strengthened beams.

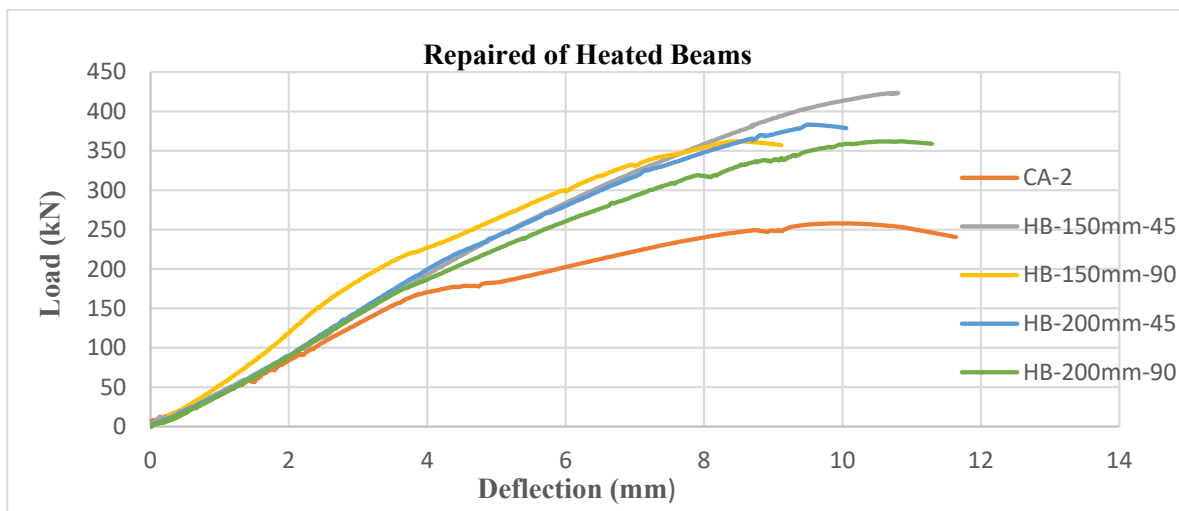


Figure 14. Enhancement ratios for the strengthened beam relative to the control beam CA-1.

4.2. Effect of NSM-CFRP Ropes on the Heated Damaged Beams

This study aims to investigate the shear strength of RC deep beams subjected to a 650 °C temperature for three hours. The effects of heat on a beam's ultimate load capacity were reduced by 20%. The shear behavior of the RC deep beams is impacted as a result of exposure to heat. The original strength of the beams was restored, and was even accompanied by an increment in strength to a point where it exceeded the strength of the unheated control beam CA-1. The ultimate capacity of the repaired heated damaged beams conveyed a rise in the ultimate capacity compared to the control beam CA-2 by 64.6%, 49%, 40.8%, and 40.8% for HB-150mm@45°, HB-200mm@45°, HB-150mm@90°, HB-200mm@90° respectively. Furthermore, shear failure was the most common failure mechanism in all repaired specimens. Figure 15 shows the load-deflection curve for repaired heated damaged beams.

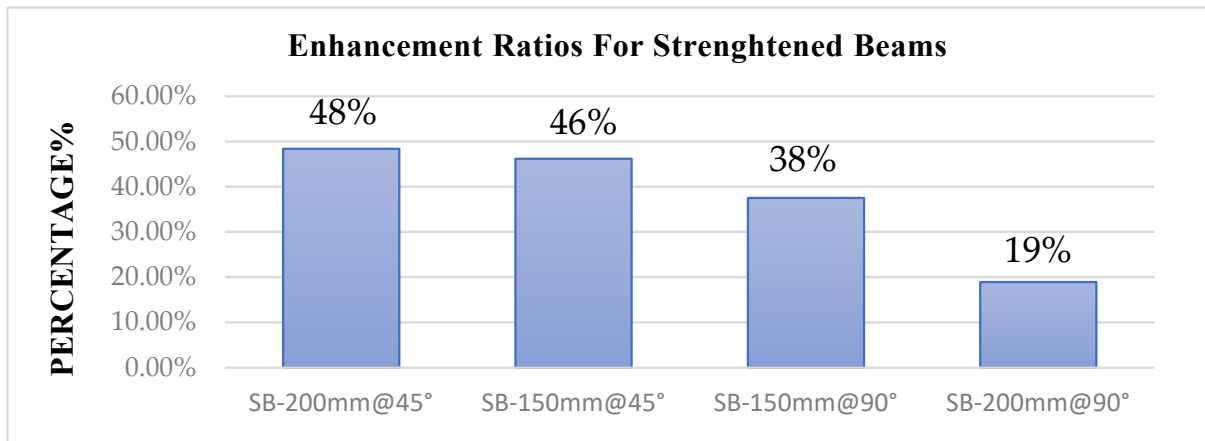


Figure 15. The load-deflection curve for repaired heated damaged beams.

As illustrated in Figure 16, the ultimate load capacity was succeeded with beam HB-150mm-45° which achieved the best repairing scheme at an enhancement ratio of 64.6%, whereas the CFRP ropes were oriented at 45° at a spacing of 150 mm. On the contrary, beam HB-150mm-90° and beam HB-200mm-90° with an enhancement ratio of 40.8% oriented at 90° to a spacing of 150 mm and 200 mm, respectively, had the lowest repairing result, although they also kept a positive increase to the overall strength of the beam. Consequently, repairing and utilizing CFRP ropes improved the ductility behavior in beam HB-150mm-90° and beam HB-200mm-90° as there was an increase in vertical deflection compared to the control beam CA-2. According to Figure 16, the enhancement ratio has been observed in repaired beams compared to the control beam CA-2 as follows: 64.6%, 49%, 40.8%, and 40.8% for HB-150mm@45°, HB-200mm@45°, HB-150mm@90°, and HB-200mm@90° respectively. The highest enhancement ratio was monitored to be 64.6% at beam HB-150mm-45° oriented at 45° with a spacing of 150mm. This indicates that repairing heat-damaged beams utilizing CFRP ropes oriented at 45° at a spacing of 150mm had the best outcome. It should be noted that in this particular orientation, the spacing made a difference as the spacing of 150 mm had a higher enhancement ratio compared to 200 mm spacing, indicating that at 45° orientation, installing CFRP ropes closer achieved better results. On the other hand, when CFRP ropes are oriented at 90°, the two different spacings have the same results, indicating that spacing doesn't make a difference in a 90° oriented beam. Figure 17 shows the deflection curve for all tested beams.

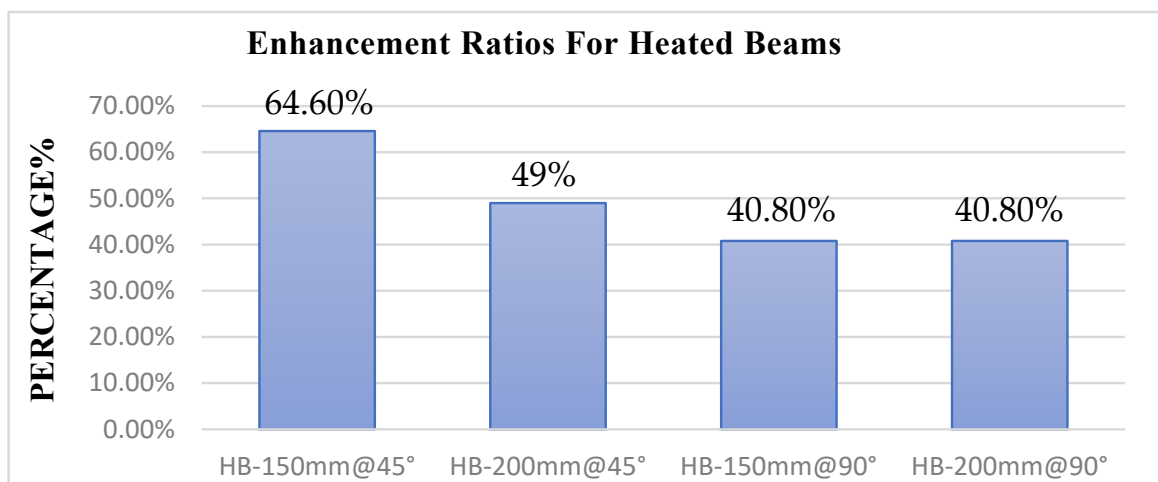


Figure 16. The enhancement ratios for heated beams relative to the control beam CA-2.

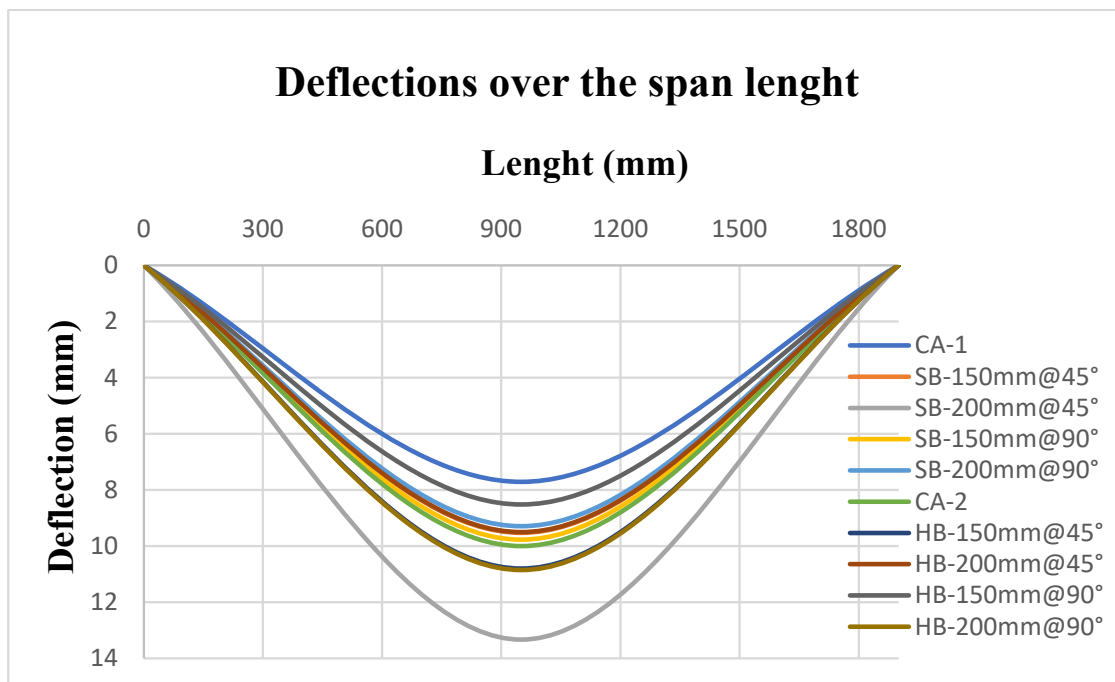


Figure 17. The deflection curve for all tested beams.

5. Conclusions

In this study, an experimental program was performed to study the shear strengthening and repairing of reinforced concrete deep beams damaged by heat utilizing near-surface mounted carbon fiber reinforced polymers (NSM-CFRP) ropes. The behavior of RC beams exposed to a high temperature of 650 °C for three hours was investigated. For this purpose, 10 RC deep beams were designed to fail in shear, and strengthened with internally bonded NSM-CFRP rope techniques using different configuration schemes. The test results given and debated throughout this study are outlined as follows:

1. The test results revealed that the internally bonded CFRP ropes approach is an efficient method for enhancing the RC deep beam's shear capacity. However, the performance depends on the orientation and spacing of the CFRP ropes along the shear span length;
2. The shear behavior of RC deep beams after being exposed to a high temperature of 650 °C for 3 h reduced the ultimate load capacity of beams by 20%;
3. The strengthened beam SB-200mm@45° in this experimental study showed the best-strengthening results with an enhancement ratio of 48% at an orientation of 45° in general, and, more specifically, at a spacing of 200 mm. In contrast, the least-strengthening results with an enhancement ratio of 19% occurred at SB-200mm@90°, which was oriented at 90° and spaced at 200 mm;
4. Among the four strengthened beams, the 45° orientation had a better result than the 90° orientation. When choosing the optimum orientation, the most economical aspect should be implemented because results from 45° or 90° orientation had satisfactory enhancement results compared to the control beam;
5. Repaired beams HB-150mm-90° and HB-200mm-90° showed the least retrofitted results with an enhancement ratio of 12% for both beams, although they still achieved satisfactory enhancement results compared to the unheated control beam CA-1.

Author Contributions: Conceptualization, M.A.-J.; methodology, A.A.; validation, A.A.-k. and A.A.; formal analysis, M.A.-J.; investigation, A.A.-k.; resources, M.A.-J.; data curation, A.A.-k.; writing—original draft preparation, A.A.-k.; writing—review and editing, A.A. and M.A.-J.; visualization, M.A.-J. and A.A.; supervision, M.A.-J.; project administration, M.A.-J. and A.A. All authors have read and agreed to the published version of the manuscript.

Funding: This research was funded by the University of Jordan.

Institutional Review Board Statement: Not applicable.

Informed Consent Statement: Informed consent was obtained from all subjects involved in this study.

Data Availability Statement: The article includes all the research data.

Acknowledgments: This work was carried out during the sabbatical leave granted to the author Mu'tasime Abdel-Jaber from the University of Jordan during the academic year 2021–2022.

Conflicts of Interest: The authors declare no conflict of interest.

References

1. Yoon, M.; Kim, G.; Choe, G.C.; Lee, Y.; Lee, T. Effect of coarse aggregate type and loading level on the high temperature properties of concrete. *Constr. Build. Mater.* **2015**, *78*, 26–33. [CrossRef]
2. Wu, Y.; Wu, B. Residual compressive strength and freeze–thaw resistance of ordinary concrete after high temperature. *Constr. Build. Mater.* **2014**, *54*, 596–604. [CrossRef]
3. Demirel, B.; Keleştemur, O. Effect of elevated temperature on the mechanical properties of concrete produced with finely ground pumice and silica fume. *Fire Saf. J.* **2010**, *45*, 385–391. [CrossRef]
4. Arioiz, O. Effects of elevated temperatures on properties of concrete. *Fire Saf. J.* **2007**, *42*, 516–522. [CrossRef]
5. Thanaraj, D.P.; Anand, N.; Arulraj, P.; Al-Jabri, K. Investigation on structural and thermal performance of reinforced concrete beams exposed to standard fire. *J. Build. Eng.* **2020**, *32*, 101764. [CrossRef]
6. Eamon, C.D.; Jensen, E. Reliability Analysis of RC Beams Exposed to Fire. *J. Struct. Eng.* **2013**, *139*, 212–220. [CrossRef]
7. Al-Zu'Bi, H.; Abdel-Jaber, M.; Katkhuda, H. Flexural Strengthening of Reinforced Concrete Beams with Variable Compressive Strength Using Near-Surface Mounted Carbon-Fiber-Reinforced Polymer Strips [NSM-CFRP]. *Fibers* **2022**, *10*, 86. [CrossRef]
8. Abdel-Jaber, M.S.; Walker, P.R.; Hutchinson, A.R. Shear strengthening of reinforced concrete beams using different configurations of externally bonded carbon fibre reinforced plates. *Mater. Struct.* **2003**, *36*, 291–301. [CrossRef]
9. Ma'en, S.; Shatanawi, A.S.; Mu'tasim, S. Guidelines for Shear Strengthening of Beams Using Carbon Fibre-Reinforced Polymer (FRP) Plates. *Jordan J. Civ. Eng.* **2007**, *1*, 327–335.
10. Hassan, S.K.H.; Abdel-Jaber, M.S.; Alqam, M. Rehabilitation of Reinforced Concrete Deep Beams Using Carbon Fiber Reinforced Polymers (CFRP). *Mod. Appl. Sci.* **2018**, *12*, 179. [CrossRef]
11. Al-Ghanem, H.; Al-Asi, A.; Abdel-Jaber, M.; Alqam, M. Shear and Flexural Behavior of Reinforced Concrete Deep Beams Strengthened with CFRP Composites. *Mod. Appl. Sci.* **2017**, *11*, 110. [CrossRef]
12. Obaidat, Y.T.; Obaidat, A.T.; Ashteyat, A.M. Behaviour of heat damaged repaired reinforced SCC cantilever beam using carbon fiber reinforced polymer rope. *Eur. J. Environ. Civ. Eng.* **2021**, *26*, 8002–8017. [CrossRef]
13. Wang, Q.; Li, T.; Zhu, H.; Su, W.; Hu, X. Bond enhancement for NSM FRP bars in concrete using different anchorage systems. *Constr. Build. Mater.* **2020**, *246*, 118316. [CrossRef]
14. Ashteyat, A.M.; Haddad, R.; Obaidat, Y.T. Repair of heat-damaged SCC cantilever beams using SNSM CFRP strips. *Structures* **2020**, *24*, 151–162. [CrossRef]
15. Al-Saadi, N.T.K.; Mohammed, A.; Al-Mahaidi, R. Performance of RC beams rehabilitated with NSM CFRP strips using innovative high-strength self-compacting cementitious adhesive (IHSSC-CA) made with graphene oxide. *Compos. Struct.* **2017**, *160*, 392–407. [CrossRef]
16. Chaliouris, C.E.; Kosmidou, P.-M.K.; Papadopoulos, N.A. Investigation of a New Strengthening Technique for RC Deep Beams Using Carbon FRP Ropes as Transverse Reinforcements. *Fibers* **2018**, *6*, 52. [CrossRef]
17. Almassri, B.; Kreit, A.; Al Mahmoud, F.; Francois, R. Behaviour of corroded shear-critical reinforced concrete beams repaired with NSM CFRP rods. *Compos. Struct.* **2015**, *123*, 204–215. [CrossRef]
18. Rizzo, A.; De Lorenzis, L. Behavior and capacity of RC beams strengthened in shear with NSM FRP reinforcement. *Constr. Build. Mater.* **2009**, *23*, 1555–1567. [CrossRef]
19. Ali, A.A.M.; Mezher, T.M. Shear Strengthening of RC without Stirrups for Deep Beams with Near Surface Mounted CFRP Rods. *Int. J. Eng. Res. Technol.* **2015**, *4*, 545–547. Available online: <https://www.researchgate.net/publication/301803232> (accessed on 9 April 2023).
20. Bianco, V.; Monti, G.; Barros, J. Design formula to evaluate the NSM FRP strips shear strength contribution to a RC beam. *Compos. Part B Eng.* **2013**, *56*, 960–971. [CrossRef]
21. Hatem, M.; Samad, A.A.A.; Mohamad, N.; Inn, G.W.; Abdulqader, S. A Review on NSM-CFRP technique using in Shear Strengthening of RC Deep Beams. *Indian J. Sci. Technol.* **2019**, *12*, 1–17. [CrossRef]
22. Ibrahim, M.; Wakjira, T.; Ebead, U. Shear strengthening of reinforced concrete deep beams using near-surface mounted hybrid carbon/glass fibre reinforced polymer strips. *Eng. Struct.* **2020**, *210*, 110412. [CrossRef]
23. Abdallah, M.; Al Mahmoud, F.; Khelil, A.; Mercier, J.; Almassri, B. Assessment of the flexural behavior of continuous RC beams strengthened with NSM-FRP bars, experimental and analytical study. *Compos. Struct.* **2020**, *242*, 112127. [CrossRef]

24. Abdel-Jaber, M.E.; Abdel-Jaber, M.T.; Katkhuda, H.; Shatarat, N.; El-Nimri, R. Influence of Compressive Strength of Concrete on Shear Strengthening of Reinforced Concrete Beams with Near Surface Mounted Carbon Fiber-Reinforced Polymer. *Buildings* **2021**, *11*, 563. [[CrossRef](#)]
25. Dias, S.; Barros, J. Shear strengthening of RC T-section beams with low strength concrete using NSM CFRP laminates. *Cem. Concr. Compos.* **2010**, *33*, 334–345. [[CrossRef](#)]
26. Jalali, M.; Sharbatdar, M.K.; Chen, J.-F.; Alaei, F.J. Shear strengthening of RC beams using innovative manually made NSM FRP bars. *Constr. Build. Mater.* **2012**, *36*, 990–1000. [[CrossRef](#)]
27. Mansour, M.; El-Maaddawy, T. Testing and modeling of deep beams strengthened with NSM-CFRP reinforcement around cutouts. *Case Stud. Constr. Mater.* **2021**, *15*, e00670. [[CrossRef](#)]
28. Al-Issawi, A.S.H.; Kamonna, H. Experimental study of RC deep beams strengthened by NSM steel bars. *Mater. Today Proc.* **2019**, *20*, 540–547. [[CrossRef](#)]
29. Albidah, A.; Abadel, A.; Abbas, H.; Almusallam, T.; Al-Salloum, Y. Experimental and analytical study of strengthening schemes for shear deficient RC deep beams. *Constr. Build. Mater.* **2019**, *216*, 673–686. [[CrossRef](#)]
30. Papadopoulos, N.A.; Naoum, M.C.; Sapidis, G.M.; Chalioris, C.E. Cracking and Fiber Debonding Identification of Concrete Deep Beams Reinforced with C-FRP Ropes against Shear Using a Real-Time Monitoring System. *Polymers* **2023**, *15*, 473. [[CrossRef](#)]
31. Karayannis, C.G.; Goliias, E.; Naoum, M.C.; Chalioris, C.E. Efficacy and Damage Diagnosis of Reinforced Concrete Columns and Joints Strengthened with FRP Ropes Using Piezoelectric Transducers. *Sensors* **2022**, *22*, 8294. [[CrossRef](#)] [[PubMed](#)]
32. Goliias, E.; Zaprís, A.G.; Kytinou, V.K.; Osman, M.; Koumtzis, M.; Siapera, D.; Chalioris, C.E.; Karayannis, C.G. Application of X-Shaped CFRP Ropes for Structural Upgrading of Reinforced Concrete Beam–Column Joints under Cyclic Loading—Experimental Study. *Fibers* **2021**, *9*, 42. [[CrossRef](#)]
33. Ji, G.; Li, G.; Alaywan, W. A new fire resistant FRP for externally bonded concrete repair. *Constr. Build. Mater.* **2013**, *42*, 87–96. [[CrossRef](#)]
34. Al-Rousan, R.; Al-Tahat, M. An Anchoring Groove Technique to Enhance the Bond Behavior between Heat-Damaged Concrete and CFRP Composites. *Buildings* **2020**, *10*, 232. [[CrossRef](#)]
35. Ahmed, A.; Kodur, V. The experimental behavior of FRP-strengthened RC beams subjected to design fire exposure. *Eng. Struct.* **2011**, *33*, 2201–2211. [[CrossRef](#)]
36. Kodur, V.; Agrawal, A. An approach for evaluating residual capacity of reinforced concrete beams exposed to fire. *Eng. Struct.* **2016**, *110*, 293–306. [[CrossRef](#)]
37. Petkova, D.; Donchev, T.; Wen, J. Experimental study of the performance of CFRP strengthened small scale beams after heating to high temperatures. *Constr. Build. Mater.* **2014**, *68*, 55–61. [[CrossRef](#)]
38. Zhai, Y.; Deng, Z.; Li, N.; Xu, R. Study on compressive mechanical capabilities of concrete after high temperature exposure and thermo-damage constitutive model. *Constr. Build. Mater.* **2014**, *68*, 777–782. [[CrossRef](#)]
39. Jiangtao, Y.; Yichao, W.; Kexu, H.; Kequan, Y.; Jianzhuang, X. The performance of near-surface mounted CFRP strengthened RC beam in fire. *Fire Saf. J.* **2017**, *90*, 86–94. [[CrossRef](#)]
40. Al-Rousan, R.Z. Impact of elevated temperature and anchored grooves on the shear behavior of reinforced concrete beams strengthened with CFRP composites. *Case Stud. Constr. Mater.* **2021**, *14*, e00487. [[CrossRef](#)]
41. American Concrete Institute. *318-19 Building Code Requirements for Structural Concrete and Commentary*; American Concrete Institute: Farmington Hills, MI, USA, 2019. [[CrossRef](#)]
42. Zhang, N.; Tan, K.-H. Direct strut-and-tie model for single span and continuous deep beams. *Eng. Struct.* **2007**, *29*, 2987–3001. [[CrossRef](#)]
43. Ismail, K.S.; Guadagnini, M.; Pilakoutas, K. Strut-and-Tie Modeling of Reinforced Concrete Deep Beams. *J. Struct. Eng.* **2018**, *144*, 04017216. [[CrossRef](#)]
44. Chen, H.; Yi, W.-J.; Hwang, H.-J. Cracking strut-and-tie model for shear strength evaluation of reinforced concrete deep beams. *Eng. Struct.* **2018**, *163*, 396–408. [[CrossRef](#)]
45. Park, J.-W.; Kuchma, D. Strut-and-Tie Model Analysis for Strength Prediction of Deep Beams. *ACI Struct. J.* **2007**, *104*, 657. [[CrossRef](#)]

Disclaimer/Publisher’s Note: The statements, opinions and data contained in all publications are solely those of the individual author(s) and contributor(s) and not of MDPI and/or the editor(s). MDPI and/or the editor(s) disclaim responsibility for any injury to people or property resulting from any ideas, methods, instructions or products referred to in the content.